Journal of South American Earth Sciences 40 (2012) 38–52

Contents lists available at SciVerse ScienceDirect

Journal of South American Earth Sciences

journal homepage: www.elsevier.com/locate/jsames

Mineral chemistry and geothermometry using relict primary minerals in the La Cocha ultramafic body: A slice of the upper mantle in the Sierra Chica of Córdoba, Sierras Pampeanas, Argentina

Patricia A. Anzil [1], Alina B. Guereschi, Roberto D. Martino*

Centro de Investigaciones en Ciencias de la Tierra (CICTERRA, CONICET-UNC), Departamento de Geología Básica, Facultad de Ciencias Exactas, Físicas y Naturales, Universidad Nacional de Córdoba, Av. Vélez Sársfield 1611, Ciudad Universitaria, Córdoba X5016GCA, Argentina

ARTICLE INFO

Article history:
Received 9 January 2012
Accepted 27 September 2012

Keywords:
Ultramafic rocks
Mineral chemistry
Geothermometry
Upper mantle
Sierras Pampeanas
Argentina

ABSTRACT

The La Cocha ultramafic body, in the Sierra Chica of Córdoba (Sierras Pampeanas, Argentina), is formed by serpentinized spinel harzburgites, with lenses of spinel pyroxenites and hornblendites. The associated metamorphic rocks are garnet sillimanite gneisses, intercalated with tabular bodies of pyroxene amphibolites and forsterite marbles.

Mineral chemistry of relict primary phases (olivine, orthopyroxene and spinel) from samples of the spinel harzburgites and pyroxenites was determined, and several geothermometers were applied to estimate the temperature conditions under which these rocks may have been equilibrated.

In the spinel harzburgites, the primary spinel is Al–chromite [Cr# = Cr/(Cr + Al) = 0.48–0.57], which is replaced by ferrichromite and chlinoclore by metamorphism. Orthopyroxene is enstatite (En_{92}) and olivine is classified as forsterite (Fo_{92}); this last one shows a homogeneous and constant composition along the ultramafic body. Using geothermometric calibrations of the pair olivine–spinel, the highest temperature of 1157 °C would correspond to the primary conditions of formation of the harzburgites.

The spinel pyroxenites show a mineral composition defined by orthopyroxene (En_{85}, enstatite), olivine (Fo_{86}, chrysolite), spinel (*s. s.*) and magnetite. Serpentine and clinochlore were produced by metamorphism. Spinel has high concentrations in Al and very low in Cr, and is classified as spinel *sensu stricto*; magnetite replacement was produced by metamorphism. Orthopyroxene and olivine are depleted in MgO regarding these minerals in the harzburgites. Temperatures of 785–734 °C calculated using geothermometers with orthopyroxene are interpreted to be produced by metamorphism in amphibolite to granulite facies conditions.

Cumular textures were not observed in outcrops and thin sections of the studied rocks. The narrow composicional range and high forsterite content in olivine, the high Cr# in spinel, and the low concentrations of Ni and Cr in whole rock analyses indicate a mantle residual origin for these peridotites, which would exclude a cumular origin.

The association of peridotites with mafic bodies formed in an N-type MORB environment and a relict mantle fabric showed by the elongated crystals/aggregates of olivine (preserved in pseudomorphic replacements), indicating a high temperature flow, allow to interpret the La Cocha ultramafic body as a slice of oceanic mantle, belonging to basal tectonites of an ophiolite complex. This body shows similar petrological, geochemical and structural features than the other ultramafic bodies in the Sierras de Córdoba, therefore the origin proposed here could be applied to the other bodies.

© 2012 Elsevier Ltd. All rights reserved.

* Corresponding author. Departamento de Geología Básica, Facultad de Ciencias Exactas, Físicas y Naturales, Universidad Nacional de Córdoba, Av. Vélez Sársfield 1611, Ciudad Universitaria, Córdoba X5016GCA, Argentina. Tel.: +54 351 4344980x115; fax: +54 351 4334139.
E-mail address: rdmartino@com.uncor.edu (R.D. Martino).
[1] Present address: Comisión Nacional de Energía Atómica, Gerencia de Exploración de Materias Primas, Regional Centro, Córdoba, Argentina.

0895-9811/$ – see front matter © 2012 Elsevier Ltd. All rights reserved.
http://dx.doi.org/10.1016/j.jsames.2012.09.009

RESUMEN

El cuerpo ultramáfico de La Cocha, en la Sierra Chica de Córdoba (Sierras Pampeanas, Argentina), está formado por harzburgitas espinélicas serpentinizadas, con lentes de piroxenitas espinélicas y hornblenditas. Las rocas metamórficas asociadas son gneises granatíferos sillimaníticos, intercalados con cuerpos tabulares de anfibolitas piroxénicas y mármoles forsteríticos.

Se realizaron los primeros análisis de química mineral de muestras de las harzburgitas espinélicas, que contienen las fases primarias de las peridotitas (olivino, ortopiroxeno y espinelo), y de las piroxenitas espinélicas, y se aplicaron varios geotermómetros para estimar las condiciones de formación.

En las harzburgitas espinélicas, el espinelo primario es una cromita rica en Al [#Cr = Cr/(Cr + Al) = 0.48 − 0.57], que por metamorfismo es reemplazado por ferricromita y clinocloro. El ortopiroxeno es enstatita (En_{92}) y el olivino se clasifica como forsterita (Fo_{92}), este último con una composición homogénea y constante a lo largo del cuerpo. Usando el par olivino–espinelo como geotermómetro, la temperatura más alta calculada de 1157 °C correspondería a las condiciones primarias de formación de las harzburgitas.

Las piroxenitas espinélicas poseen una composición mineral definida por ortopiroxeno (En_{85}, enstatita), olivino (Fo_{86}, crisolita), espinelo (*s. s.*) y magnetita. Serpentina y clinocloro son producto del metamorfismo. El espinelo tiene concentraciones altas de Al y muy bajas de Cr, y se clasifica como espinelo *sensu stricto*; reemplazos por magnetita son producto del metamorfismo. El ortopiroxeno y el olivino están empobrecidos en MgO en relación con las harzburgitas. Temperaturas de 785–734 °C calculadas usando geotermómetros con ortopiroxeno son interpretadas como producto de metamorfismo en condiciones de facies de anfibolitas a granulitas.

No se observaron texturas cumulares en los afloramientos y secciones delgadas de las rocas estudiadas. El estrecho rango composicional y la elevada concentración en forsterita que posee el olivino, el alto #Cr del espinelo, y las bajas concentraciones de Ni y Cr en los análisis químicos de roca total serían indicadores de un origen residual del manto para las peridotitas, que descartarían un origen cumular para estas rocas.

La asociación de las peridotitas con cuerpos máficos formados en un ambiente tipo N-MORB y la fábrica mantélica relíctica de los cristales/agregados de olivino (preservada en los reemplazos pseudomórficos), indicando un flujo de alta temperatura, permiten interpretar al cuerpo ultramafico La Cocha como una escama de manto oceánico, correspondiente a tectonitas basales de un complejo ofiolítico. Dado que este cuerpo posee similares características petrológicas, geoquímicas y estructurales que los otros cuerpos ultramáficos de las Sierras de Córdoba, el origen propuesto aquí podría aplicarse a los otros cuerpos.

© 2012 Elsevier Ltd. All rights reserved.

1. Introduction

Mineral chemistry of ultramafic rocks can provide useful information about the environment in which these rocks could be originated. In spite of the high degree of serpentinization and deformation, both by mantle flow and by orogenic processes, the compositions of the relict primary minerals in the peridotites, mainly spinel and olivine, are still preserved and provide important information about the physical conditions of its origin and in some cases of the tectonic environment (Dick and Bullen, 1984; Arai, 1994a; Roeder, 1994; Barnes and Roeder, 2001; Kamenetsky et al., 2001; Metzger et al., 2002; Coish and Gardner, 2004; Ahmed et al., 2005). Temperature conditions under which these rocks may have been equilibrated can be established by means of the application of a classic geothermometry, but they often lack pressure index minerals.

Mineral chemistry of spinel is particularly important: it is the most reliable petrogenetic indicator (Irvine, 1965, 1967) because in most cases it survives metamorphism, which allows to preserve the primary conditions. Mineral chemistry is sensitive to whole rock composition, mineral association, and conditions of pressure, temperature and oxygen fugacity (Irvine, 1965).

In upper mantle peridotites, the composition of spinel, mainly the Cr-number [Cr# = Cr/(Cr + Al)], can indicate the degree of partial melting and has been used as a guide to classify the peridotites in terms of tectonic environments (Dick and Bullen, 1984; Arai, 1994a). The degree of partial melting, including second-stage melting (Duncan and Green, 1980), enhances the Cr# of spinel in the peridotite restite (Dick and Bullen, 1984; Arai, 1994a). The melting style of the upper mantle is possibly different from a tectonic setting to another, with different degrees of melting in peridotites from arcs, plumes and mid-ocean ridges (Dick and Bullen, 1984; Arai, 1994a). Depleted peridotite with high Cr# (>0.7) in spinel can be produced either at the mantle wedge beneath arcs or at the plume-related within-plate mantle (Pearce et al., 1984; Arai, 1994b; Ishiwatari et al., 2003). The TiO_2 content of spinel varies depending on the tectonic place of generation: it is the lowest for the arc magmas, intermediate for MORB and the highest for intraplate magmas (Arai, 1992). For these properties, Cr, Fe and Ti are the main elements in the mineral chemistry of spinel that are used in the tectonic discrimination diagrams for peridotites.

Subsolidus equilibration during metamorphic or hydrothermal processes can significantly modify the primary composition of spinel (Abzalov, 1998; Mellini et al., 2005; Gervilla et al., 2012); therefore, the use of their chemical composition as a petrogenetic and geotectonic indicator needs a careful petrographic study.

The ultramafic rocks of the La Cocha body in the Sierra Chica of Córdoba (Sierras Pampeanas, Argentina) preserve relics of the original mineral assemblage, mainly spinel, olivine and orthopyroxene. These rocks has been studied in their petrological and whole rock geochemical features (Pugliese, 1995; Escayola et al., 1996; Pugliese and Villar, 2001, 2002, 2004; Anzil and Martino, 2009b), however the results reported here are the first studies of mineral chemistry and geothermometry using relict primary minerals carried out in these rocks.

The objectives of this contribution are the following ones: (a) to characterize the mineral chemistry of the La Cocha ultramafic rocks

in the Sierra Chica of Córdoba, (b) to perform geothermometric calculations in order to establish the temperature conditions of formation of these rocks, (c) to interpret their origin and evolution, and (d) to compare it with the thermotectonic evolution of the associated metamorphic rocks in the Sierra Chica, established by Martino et al. (2010), and representative of the Pampean orogen in the Sierras de Córdoba at this latitude.

2. Geological setting

The Sierras de Córdoba (Fig. 1) is the easternmost group of the Sierras Pampeanas of Argentina and encompasses a ~500 km long and ~150 km wide area. They consist of several north-trending ranges composed of a Neoproterozoic–Early Paleozoic polydeformed metamorphic basement (Pampean Orogenic Cycle, ~530 Ma; Rapela et al., 1998; Siegesmund et al., 2010), imbricated by contractional ductile shear zones of Middle to Late Paleozoic ages (Martino, 2003), and intruded by Paleozoic granitoids (Famatinian Orogenic Cycle; Rapela et al., 1998). These ranges are limited by Tertiary west-vergent reverse faults and separated by Mesozoic to Cenozoic intermontane sediments. The east-tilted basement blocks were uplifted during the Andean Orogenic Cycle and are surrounded by the Quaternary Chaco–Pampean plain. Neogene trachyandesites and pyroclastic deposits partly cover the basement rocks in the western side.

In the polydeformed metamorphic basement, a regional granulite facies thermal axis of Early Cambrian migmatites is recognized (Fig. 1; Martino et al., 1995, 1997, 1999). Minor outcrops of Neoproterozoic ultramafic rocks (647 ± 77 Ma, Sm–Nd in ophiolite remnants, Escayola et al., 2007) are recognized in the Sierra Grande and the Sierra Chica (Villar, 1975; Escayola et al., 1996). These rocks have been interpreted as forming part of possible sutures of terranes accreted to the Gondwana margin during the Neoproterozoic–Early Paleozoic (Kraemer et al., 1995; Ramos et al., 2000; Escayola and Kraemer, 2003). Based on local and regional structural relationships, Martino et al. (2010) interpreted that the Sierra Chica ultramafic bodies were emplaced as upper mantle slices in an accretionary prism that was reworked during the Cambrian Pampean orogeny.

3. The La Cocha ultramafic body

The studied area cover the La Cocha hill (31° 36′ 40″ LS–64° 32′ 40″ LO, 1250 m a.s.l., Fig. 2), located ~10 km toward the northwest of the Alta Gracia city, mainly in the Central Sierra Chica (Fig. 1). In this place, an ultramafic body elongated toward the northeast, ~500 m long and ~200 m wide, crops out.

The ultramafic body is associated with metamorphic rocks, dominantly composed of garnet sillimanite gneisses, with intercalations of tabular bodies of two pyroxene amphibolites (Anzil and Martino, 2012). In the core of the ultramafic body, tabular bodies (<200 m long) of forsterite marbles and non-pyroxene amphibolites are recognized. The metamorphic rocks develop a foliation under high-grade conditions (Martino et al., 2010). On the whole, all these rocks define a major low cylindricity recumbent fold, with the axis plunging with high-angle to the north (N 20°/68°) and the axial plane striking NNE and dipping with high-angle to the east (N 10°/85° E; Anzil, 2009; Anzil and Martino, 2009a; Martino et al., 2010). This structure would be part of a large sheath fold, now partially eroded. In the surroundings of the studied area, several ultramafic bodies with similar petrographic and structural features were recognized (Anzi,l 2009; Martino et al., 2010).

The La Cocha ultramafic body (Fig. 2) is essentially composed of partially to totally serpentinized spinel harzburgites (serpentinites). An internal foliation defined by a compositional layering (Fig. 3a) is recognized in all the ultramafic body (Anzil and Martino, 2009a; Martino et al., 2010). In the core of the ultramafic body, decametric lenses (<20 cm wide) of hornblendites and spinel pyroxenites are recognized, the last associated with chromitite layers (nowadays totally removed by mining), concordant with the internal foliation of ultramafic rocks. The hornblendite layers also occur in the contact of the ultramafic body with the amphibolites. The dominant spinel harzburgites and the associated spinel pyroxenites lenses are the main rocks studied in this work.

3.1. Spinel harzburgites

The spinel harzburgites were determined by modal classifications estimated from petrography of relict primary minerals and pseudomorphic replacements (Anzil, 2009; Anzil and Martino, 2009a). The rocks are dark green, foliated, and with reddish lenses (<2 cm wide). A fine grained (<1 mm long) elongated granular matrix is dominantly composed of serpentinized olivine (70–80% of the rock). Reddish isolated crystals (<4 mm long) or aggregates of orthopyroxene (20–30%), partially to completely bastitized, give a general porphyritic look to the rock. The accessory phases (<2%) are minerals of the spinel group. Products of replacement are minerals of the serpentine group, chlorite group, Ca-amphiboles, calcite and Fe-oxides.

A compositional layering (<2 cm wide, Fig. 3a) is defined by the elongation and irregular concentration of lens-like pyroxene layers that alternate with more regular, elongated granular aggregates of olivine layers. Intrafolial microfolds of bastitized pyroxene aggregates were also identified. This internal foliation is interpreted as a high temperature mantle foliation (Anzil, 2009; Anzil and Martino, 2009a; Martino et al., 2010). This foliation is cut by an axial plane foliation (Anzil, 2009; Anzil and Martino, 2009a; Martino et al., 2010), filled by fibrous serpentine and tremolite veins (amphibolitization; Anzil and Martino, 2009b).

Different replacement assemblages in the ultramafic rocks were identified based on textural relationships, mineral chemistry and X-ray diffraction in minerals of the serpentine group by Anzil (2009) and Anzil and Martino (2009b). According to the degree of alteration, three types of serpentinized rocks are distinguished: (a) with presence of primary minerals of the peridotites, (b) totally serpentinized, and (c) those affected by amphibolitization. The (a) serpentinized spinel harzburgites with relics of primary minerals as olivine, orthopyroxene and reddish brown spinel are studied in this work.

In thin section, mesh and bastitic textures suggest pseudomorphic replacements (Gervilla, 1997). Olivine (<1 mm long) is partially to completely serpentinized (lizardite) from the edge to the core, displaying typical mesh textures that leave olivine relicts; when these relicts are also replaced, hourglass and window textures occur (Deer et al., 1992). The latter texture is defined by a single green yellow tabular serpentine crystal in the middle of the replaced olivine crystal, oriented with (001) perpendicular to the foliation. Magnetite rims mark the old crystal contours. Orthopyroxene (<4 mm long) is pink to pale green, partially to totally replaced by serpentine, forming centimeter-long bastites with magnetite along fractures and edges; cleavage usually is parallel to the foliation.

The main accessory phase is a reddish brown spinel (<0.5 mm long, Fig. 3b) forming isolated grains or aggregates parallel to the foliation, although scarce green spinel occurs in a few samples without reddish brown spinel. Isolated grains of magnetite are also recognized. Clinochlore occurs as scarce sheets disseminated in the serpentine matrix and forming coronas around minerals of the spinel group. Amphibole occurs as long crystals disseminated in the serpentine matrix and also filling veins (tremolite).

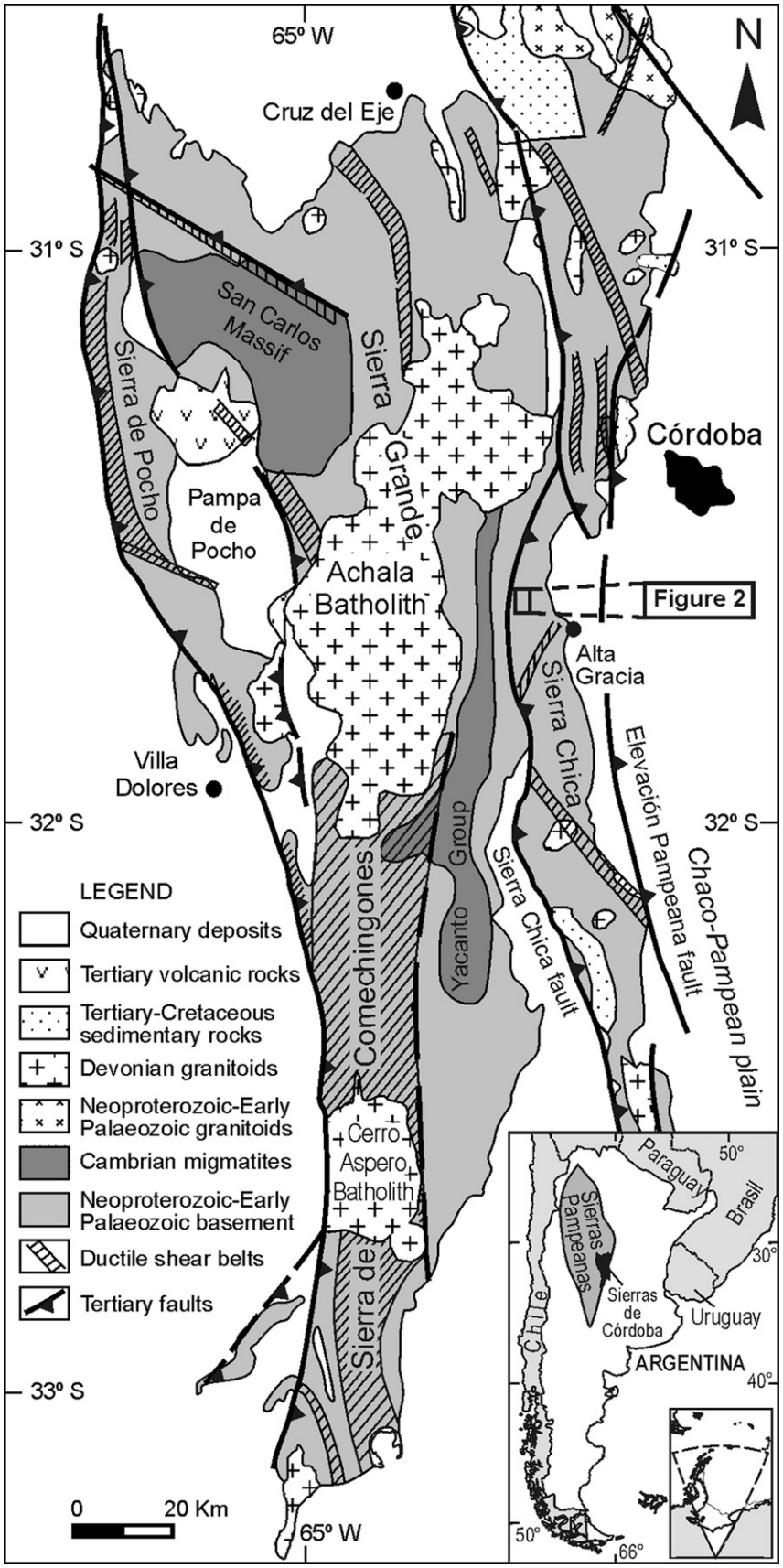

Fig. 1. Geological map of the Sierras de Córdoba, including the studied area in the Sierra Chica.

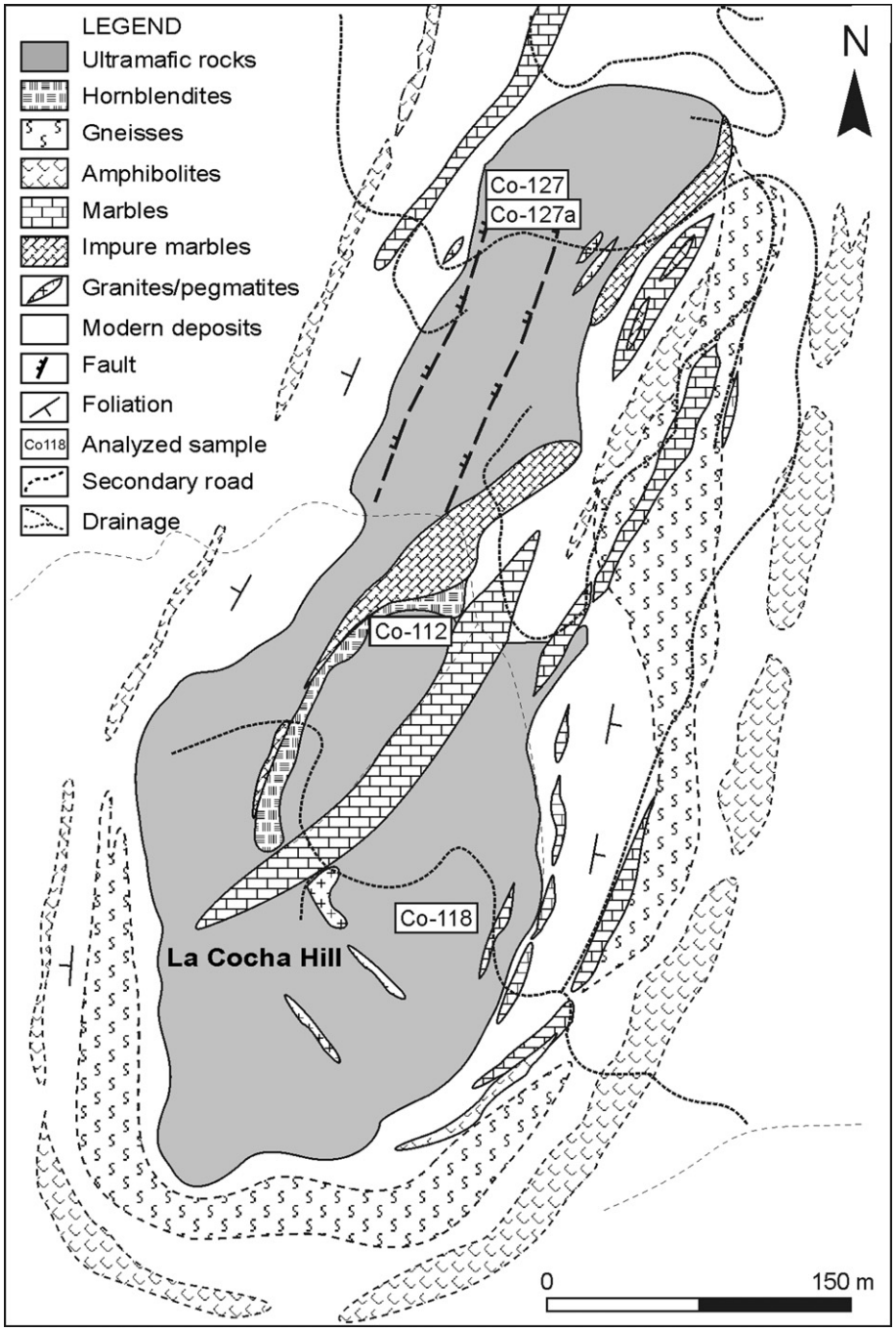

Fig. 2. Geological map of the La Cocha ultramafic body.

Fibrous serpentine veins that cut the internal foliation are of non asbestiform type, with columnar texture (Wicks and Whittaker, 1977) and the fibers oriented perpendicular to the wall. They are classified as lizardite 1T by optic methods and X ray diffraction (Anzil and Martino, 2009b).

3.2. Spinel pyroxenites lenses

The spinel pyroxenites are fine grained black rocks, with abundant magnetic minerals (magnetite). Centimetric talc-rich veins give a shiny look to the rock. In detail, millimetric lenses of magnetite and green spinel (~35% of the rock) are distinguished from a fine grained (<1 mm) reddish granular matrix (~65% of the rock) composed of partially serpentinized pyroxene and olivine. Orthopyroxene is pale pink and forms euhedral short prisms (<0.5 mm long); in general, it is not altered. Olivine is colorless, rounded (<1 mm) and, in general, strongly fractured and crossed by serpentine veins. Spinel is green and euhedral (<0.5 mm, Fig. 3c), with exsolution of an opaque mineral (probably magnetite) in the core (Fig. 3d); in places, opaque grains are elongated and arranged in thin strips. Very abundant magnetite forms isolated grains (<2 mm) and coronas around green spinel (Fig. 3d). In more altered rocks, clinochlore coronas were also developed around both magnetite and green spinel. Secondary minerals are prismatic

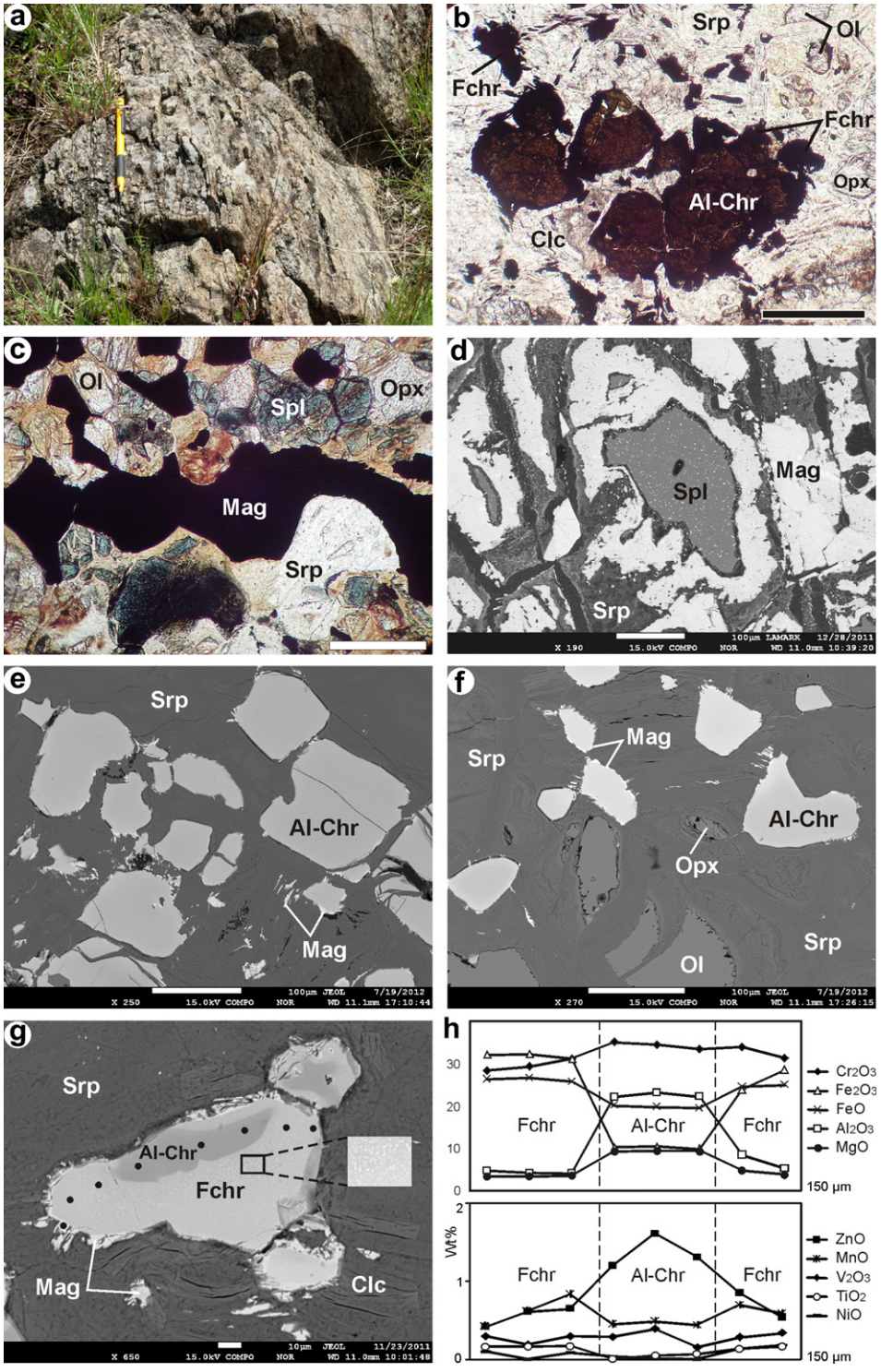

Fig. 3. **a**. Tabular outcrops of the La Cocha ultramafic rocks controlled by a mantle foliation (marked by the pencil, length = 14 cm). **b**. Photomicrograph under plane-polarized light of the spinel harzburgites composed of olivine (Ol), orthopyroxene (Opx) and Al–chromite (Al–Chr) with ferrichromite rims (Fchr), associated with clinochlore (Clc) in a serpentine matrix (Srp); scale bar = 1 mm **c**. Photomicrograph under plane-polarized light of the spinel pyroxenites composed of orthopyroxene, olivine, green spinel (Spl), magnetite (Mag) and serpentine; scale bar = 0.5 mm. **d**. Backscattered electron (BSE) image of the spinel pyroxenites showing magnetite rims around spinel *s. s.*, which also contains tiny blebs of magnetite exsolution; scale bar = 100 µm. **e**. BSE image of the spinel harzburgites showing Al–chromite grains, unaltered or only with thin magnetite rims, in a serpentine matrix; scale bar = 100 µm **f**. BSE image of the spinel harzburgites with relicts of olivine, orthopyroxene and Al–chromite in a serpentine matrix; scale bar = 100 µm. **g**. BSE image of the spinel harzburgites showing chemical zonation by alteration of an Al–chromite grain with a ferrichromite zone (with exsolutions of magnetite, see detail) and thin magnetite rims, associated with clinochlore in a serpentine matrix; the black circles are the analyzed points; scale bar = 10 µm. **h**. Compositional profiles of the analyzed points in the zoned Al–chromite grain marked in **g**.

tremolite in the matrix of the rock, and serpentine (lizardite) and talc in veins that cross all the minerals, mainly olivine.

4. Mineral chemistry

Compositional data of mineral phases of petrogenetic interest were obtained by electron probe microanalysis using a JEOL Superprobe JXA-8200 at the Departamento de Geología at the Universidad de Huelva (Spain) and a JEOL Superprobe JXA-8230 at the Laboratorio de Microscopía Electrónica y Análisis por Rayos X (LAMARX) at the Universidad Nacional de Córdoba (Argentina). Operating conditions for spot analyses were 15 kV and 20 nA; spot sizes were 2–10 μm depending on the analyzed phase. Natural minerals and synthetic oxides were used as standards: wollastonite for Si and Ca, rutile for Ti, magnetite for Fe in spinel, fayalite for Fe in olivine and pyroxene, periclase for Mg in spinel, forsterite for Mg in olivine and pyroxene, jadeite for Al and Na, orthoclase for K, rodonite for Mn and Zn, chromium oxide for Cr, skutterudite for Ni and vanadinite for V. Data were calculated using the Pouchou and Pichoir Method (1985). The ferric and ferrous irons of spinel were calculated assuming spinel stoichiometry.

After a careful petrographic study of 21 samples from the La Cocha ultramafic rocks, four representative samples were selected for microprobe analyses: two samples of the spinel harzburgites with relics of primary minerals (Co-127 and Co-127a) and one almost totally serpentinized (Co-118), and one sample of the spinel pyroxenites (Co-112). The analyzed phases were minerals of the spinel group, olivine and orthopyroxene. Representative microprobe analyses are listed in Tables 1–3.

4.1. Minerals of the spinel group

4.1.1. In the spinel harzburgites

The main accessory mineral (<2%) of the spinel group analyzed in these rocks (Table 1) is a euhedral to subhedral reddish brown grain (<0.5 mm long; Fig. 3b), with high contents of Cr_2O_3 (34–39%), FeO (28–33%) and Al_2O_3 (19–24%), and low values of MgO (7–10%). The TiO_2 content is very low (<0.2%). The Cr# varies between 0.48 and 0.57 and the Mg# between 0.31 and 0.47. This spinel is classified as **Al–chromite** [$Fe^{2+}(Cr, Al)_2O_4$]. Individual grains are homogeneous down to the resolution of the electron microprobe. The grains are unaltered or only show a very thin magnetite rim (<1 μm wide) in a serpentine matrix (Fig. 3e,f). The compositions of the different minerals of the spinel group are showed in the triangle Cr–Al–Fe^{+3} (Fig. 4).

Another phase occurs as coronas (<50 μm wide, Fig. 3b,g) around some grains of Al–chromite in the samples Co-127 and Co-127a or as isolate irregular opaque grains (<0.5 mm long) in the serpentine matrix in the more altered sample Co-118. The chemical composition is characterized by high contents of Cr_2O_3 (32–40%), Fe_2O_3 (23–31%) and FeO (24–29%), and very low of Al_2O_3 (2–4%) and MgO (2–4%). The Cr# varies between 0.82 and 0.90. This phase is classified as **ferrichromite** [$Fe^{+2}(Cr, Fe^{+3})_2O_4$], the type of chromite alteration found in many ultramafic rocks (Spangenberg, 1943; Evans and Frost, 1975). It is a submicroscopic intergrowth of oxide phases, usually enriched in FeO and Fe_2O_3, and depleted in Al_2O_3 and MgO. A range of Fe-number ($Fe\# = Fe^{2+}/(Mg + Fe^{2+}) > 0.1$ and Mg-number ($Mg\# = Mg/(Mg + Fe^{2+}) < 0.4$ is defined for ferrichromite (Bliss and MacLean, 1975; Barra et al., 1998). It is commonly accompanied by chlinoclore. Ferrichromite usually forms along chromite rims and cracks in lower grade rocks and as homogeneous grains in high-grade metamorphic rocks (Loferski and Lipin, 1983).

Al–chromite replacement extent is variable from sample to sample, increasing in sample Co-118. In samples Co-127 and Co-127a, most Al–chromite grains are unaltered or only show thin magnetite rims (<1 μm wide, Fig. 3e,f), but some grains record ferrichromite alteration in the form of textural and chemical zoning (Fig. 3g). In these composite grains, Al–chromite cores have rounded shapes and sharp contacts with ferrichromite zones (<50 μm wide), and are associated with clinochlore in a serpentine matrix. In backscattered electron images (Fig. 3g), Al–chromite is dark gray (low average atomic number); ferrichromite is light gray (medium average atomic number) and, in some places, shows exsolutions of a Fe-rich phase (white, high average atomic number), probably tiny blebs of magnetite (see detail in Fig. 3g), which also forms thin ragged rims along some edges. A sharp increase in the Fe_2O_3 and FeO contents and a decrease in the Al_2O_3 and MgO contents towards the rim are clearly recognized (Fig. 3h). The Cr_2O_3 contents remains constant or show a slight decrease from Al–chromite to ferrichromite. The ZnO contents show a continuous decrease towards the rim. The MnO, V_2O_3, TiO_2 and NiO contents show a slight increase from Al–chromite to ferrichromite.

4.1.2. In the spinel pyroxenites

Two types of minerals of the spinel group were distinguished in these rocks. The first type is a green spinel (Fig. 3c) that appears as aggregates of subhedral grains (<2 mm long) in an interstitial phase and as inclusion in orthopyroxene. It contains small blebs of an opaque mineral (probably magnetite) exsolved within the grain and/or in the rims as coronas (Fig. 3d). The exsolution of magnetite in spinel suggests an early stabilization of a solid solution of Fe-rich spinel during the cooling (Loferski and Lipin, 1983). A weak zonation is recognized in some spinel grains, with higher concentration of the exsolution in the core. The interstitial grains show sharp edges, with contacts defining triple points and fractures filled by magnetite. The chemical composition of the green spinel shows high contents of Al_2O_3 (63.4–64.4%) and MgO (18.4–19.1%), low in FeO (15.3–16.3%) and very low in Cr_2O_3 (1.2–1.6%). This mineral is classified as **spinel *sensu stricto*** ($MgAl_2O_4$), with Mg# between 0.64 and 0.72 (Table 1).

The second type of mineral of the spinel group is an opaque mineral (Fig. 3b) that commonly appear as anhedral to subhedral grains (<1 mm long). It also forms exsolutions within spinel (*s. s.*), and fills fractures and forms rims around it and olivine. The chemical composition is characterized by high contents of FeO total (91–95%) and low of Cr_2O_3 (<2.3%), MgO (<0.6%) and Al_2O_3 (<0.5%). The contents of TiO_2 (<0.9%), NiO (<0.8%) and V_2O_3 (<0.5%) are low. This composition allows to classify the analyzed opaque mineral as **magnetite** ($Fe^{2+}Fe^{3+}{}_2O_4$). The magnetite rims around spinel *s. s.* show higher contents of Al_2O_3 (2–4%) and up to 1% of MnO. The discrete grains of magnetite are associated with rounded grains of ilmenite (with 4–8% of MgO and 1–3% of MnO), which also occur as exsolution rods in magnetite.

4.2. Olivine

The olivine grains in the La Cocha spinel harzburgites are partially to totally serpentinized along edges and fractures, but unaltered relict cores are preserved (Fig. 3f). They show intragrain and intergrain chemical homogeneity of MgO (50.9–51.6%) and FeO (7.3–7.9; Table 2) contents and no significant variation within samples. The MnO content is very low (0.06–0.14%) and the NiO content is low (0.36–0.48%). Based on the $Mg/(Fe^{+2} + Mg)$ content, olivine is classified as **forsterite** (Fo_{92}).

Olivine in the spinel pyroxenites (sample Co-112), on the other hand, shows lower contents of MgO (46.5–47.1%) and FeO (12.7–13.4; Table 2) than in the spinel harzburgites, also without significant intragrain variation. The MnO (0.21–0.29%) and the NiO (0.11–0.22%) contents are low. Olivine in the spinel pyroxenites is classified as **chrysolite** (Fo_{86}).

Table 1
Representative chemical analyses (wt% oxides) of minerals of the spinel group from the La Cocha ultramafic rocks.

Sample	CO-127	CO-127	CO-127	CO-127a	CO-127a	CO-127a	CO-127a	CO-127a	CO-127	CO-127a	CO-127a	CO-118
Point	1	3	Rim_5	Core-2a	Core-2b	Core-1b	6	Core-36	2	Rim-1c	Rim-1b	Core-2
Mineral	Crhom	Crhom	Crhom	Crhom	Crhom	Crhom	Crhom	Crhom	Ferrichr	Ferrichr	Ferrichr	Ferrichr
Total number of spinel analyses $n = 70$												
SiO_2		0.004			0.01		0.003			0.004	0.001	
TiO_2		0.083	0.045	0.056	0.062	0.045	0.067		0.097	0.133	0.171	0.177
Al_2O_3	22.265	19.175	20.772	21.196	24.408	23.291	19.669	22.249	10.266	8.541	4.22	3.123
Fe_2O_3	10.533	11.785	8.228	10.283	9.458	10.588	10.606	10.395	11.399	24.040	31.401	28.514
FeO	21.792	22.337	24.511	20.744	19.753	19.947	22.741	20.278	24.860	24.741	25.953	27.338
MnO	0.434	0.468	0.405	0.505	0.327	0.487	0.149	0.45	0.591	0.696	0.831	0.328
MgO	9.099	8.418	6.984	8.827	9.945	9.625	7.967	9.466	5.66	4.796	3.637	3.471
CaO	0.006	0.007		0.018								
ZnO	0.484	0.709	0.959	1.599	1.531	1.612	1.035	1.199	0.728	0.85	0.647	0.346
Cr_2O_3	35.717	36.308	37.113	36.054	33.897	34.718	36.735	35.322	45.484	34.121	31.365	36.384
NiO	0.099	0.179	0.183		0.021	0.014	0.069	0.037	0.167	0.135	0.083	0.301
V_2O_3	0.285			0.255	0.313	0.385	0.17	0.286		0.279	0.292	0.198
Total	100.71	99.47	99.20	99.54	99.72	100.71	99.21	99.68	99.25	98.34	98.60	100.18
Number of cations on the basis of 4O												
Si		0.000			0.000		0.000			0.000	0.000	
Ti		0.002	0.001	0.001	0.001	0.001	0.002		0.003	0.004	0.005	0.005
Al	0.824	0.729	0.796	0.798	0.899	0.856	0.751	0.829	0.415	0.351	0.177	0.130
Fe3+	0.250	0.291	0.195	0.248	0.220	0.250	0.260	0.248	0.298	0.675	0.910	0.818
Fe2+	0.578	0.609	0.673	0.560	0.521	0.526	0.623	0.542	0.720	0.728	0.780	0.816
Mn	0.012	0.013	0.011	0.014	0.009	0.013	0.004	0.012	0.017	0.021	0.025	0.010
Mg	0.430	0.409	0.342	0.425	0.468	0.452	0.389	0.451	0.292	0.252	0.195	0.185
Ca	0.000	0.000		0.001								
Zn	0.011	0.017	0.023	0.038	0.036	0.038	0.025	0.028	0.019	0.022	0.017	0.009
Cr	0.887	0.926	0.954	0.911	0.838	0.856	0.941	0.883	1.233	0.940	0.882	1.016
Ni	0.003	0.005	0.005		0.001	0.000	0.002	0.001	0.005	0.004	0.002	0.009
V	0.006			0.005	0.007	0.008	0.004	0.006	0.006	0.006	0.004	
Total	3.000	3.000	3.000	3.000	3.000	3.000	3.000	3.000	3.000	3.000	3.000	3.000
Mg/Mg + Fe2	0.43	0.40	0.34	0.43	0.47	0.46	0.38	0.45	0.29	0.26	0.20	0.18
Cr/(Cr + Al)	0.52	0.56	0.55	0.53	0.48	0.50	0.56	0.52	0.75	0.73	0.83	0.89

Sample	CO-112	CO-112	CO-112	CO-112	CO-112	CO-112	CO-112	CO-112	CO-112	CO-112	CO-112	CO-112
Point	Spl-1e	Spl-3b	Incl-Opx	22	25	34	36	Mag-2	Mag-5	Mag-8	Rim-1	Rim-4
Mineral	Spinel	Spinel	Spinel	Spinel	Spinel	Spinel	Spinel	Mag	Mag	Mag	Mag	Mag
SiO_2	0.027	0.029	0.012	0.036	0.014	0.051	0.009				0.015	0.015
TiO_2	0.052	0.003	0	0.016	0.021	0.020		0.152	0.353	0.405		
Al_2O_3	62.265	63.644	59.919	63.977	63.590	63.684	63.437	0.473	0.564	0.570	3.389	3.389
Fe_2O_3			1.938	2.670	3.096	2.079	2.846	63.670	64.169	64.004	61.292	61.292
FeO	17.485	15.021	15.795	13.958	13.087	13.507	13.242	30.756	30.789	31.520	31.447	31.447
MnO	0.188	0.18	0.072	0.135	0.187	0.148	0.144	0.048	0.077	0.091	1.066	1.066
MgO	17.086	17.5	17.964	18.438	18.876	18.511	18.676	0.541	0.639	0.562	0.318	0.318
CaO	0.014	0.004	0.000	0.005	0.017	0.014	0.023		0.003			
ZnO	0.222	0.348	0.338					0.049	0.146	0.088	0.313	0.313
Cr_2O_3	2.403	2.183	4.411	1.150	1.360	1.481	1.438	2.328	1.696	1.751	1.783	1.783
NiO	0.232	0.217	0.106	0.245	0.230	0.202	0.277	0.227	0.079	0.037	0.040	0.040
V_2O_3			0.000	0.059	0.065	0.010	0.056	0.496	0.574	0.356	0.092	0.092
Total	99.97	99.13	100.56	100.70	100.59	99.72	100.19	0.77	99.09	99.38	99.76	99.76
Number of cations on the basis of 4O												
Si	0.001	0.001	0.000	0.001		0.001					0.001	0.001
Ti	0.001	0.000	0.000					0.004	0.010	0.011		
Al	1.891	1.924	1.832	1.919	1.908	1.924	1.911	0.020	0.024	0.024	0.142	0.142
Fe^{3+}			0.018	0.051	0.059	0.040	0.055	1.918	1.925	1.913	1.804	1.804
Fe^{2+}	0.381	0.325	0.346	0.297	0.279	0.290	0.283	0.943	0.940	0.959	0.943	0.943
Mn	0.004	0.004	0.002	0.003	0.004	0.003	0.003	0.001	0.002	0.003	0.032	0.032
Mg	0.663	0.676	0.702	0.700	0.716	0.707	0.712	0.030	0.035	0.030	0.017	0.017
Ca	0.000	0.000	0.000				0.001		0.000			
Zn	0.004	0.007	0.007					0.001	0.004	0.002	0.008	0.008
Cr	0.049	0.044	0.090	0.023	0.027	0.030	0.029	0.067	0.048	0.050	0.050	0.050
Ni	0.005	0.005	0.002	0.005	0.005	0.004	0.006	0.007	0.002	0.001	0.001	0.001
V			0.000	0.001	0.001	0.000	0.001	0.008	0.009	0.006	0.002	0.002
Total	2.999	2.985	3.000	3.001	3.001	3.001	3.002	3.000	3.000	3.000	3.000	3.000
$Mg/(Mg + Fe^{2+})$	0.64	0.68	0.67	0.70	0.72	0.71	0.72	0.03	0.04	0.03	0.02	0.02
Cr/(Cr + Al)	0.03	0.02	0.05	0.01	0.01	0.02	0.01	0.77	0.67	0.67	0.26	0.26

Detection limits (ppm): Si = 96, Ti = 125, Mn = 217, Ca = 78, Zn = 450, Ni = 159, V = 249.

Table 2
Representative chemical analyses (wt% oxides) of olivine from the La Cocha ultramafic rocks.

Sample	CO-127a	CO-127a	CO-127a	CO-127a	CO-127	CO-127	CO-118	CO-118	CO-118	CO-112	CO-112	CO-112
Point	9	10	39	40	14	18	4	5	8	1	2	18
Total number of olivine analyses $n = 39$												
SiO_2	40.358	40.456	40.382	40.239	40.706	40.488	40.735	40.763	40.539	39.547	39.753	39.612
TiO_2	0.006	0.007	0.003	0.02	0.003	0.018	0.014				0.012	0.002
Al_2O_3		0.039		0.03		0.007	0.018			0.001	0.014	0.01
FeO	7.393	7.333	7.31	7.415	7.823	7.943	7.374	7.518	7.321	13.038	13.194	13.361
MnO	0.12	0.099	0.106	0.111	0.127	0.111	0.104	0.111	0.07	0.293	0.221	0.233
MgO	50.59	50.091	50.496	51.001	51.359	51.523	51.704	51.772	51.559	47.128	46.713	46.945
CaO	0.034	0.014	0.003	0.023	0.004		0.005	0.032	0.036	0.01	0.023	0.014
Cr_2O_3	0.233	0.061	0.065			0.003		0.19				
NiO	0.389	0.447	0.465	0.459	0.459	0.392	0.368	0.484	0.487	0.163	0.137	0.181
V_2O_3		0.044	0.016		0.019	0.026			0.015		0.034	
Total	99.12	98.59	98.85	99.30	100.50	100.51	100.32	100.87	100.07	100.18	100.10	100.36
Number of cations on the basis of 4O												
Si	0.990	0.996	0.993	0.986	0.987	0.982	0.987	0.984	0.985	0.985	0.990	0.986
Ti	0.000	0.000	0.000	0.000	0.000	0.000	0.000				0.000	0.000
Al		0.001		0.001		0.000	0.001			0.000	0.000	0.000
Fe^{2+}	0.152	0.151	0.150	0.152	0.159	0.161	0.149	0.152	0.149	0.271	0.275	0.278
Mn	0.002	0.002	0.002	0.002	0.003	0.002	0.002	0.002	0.001	0.006	0.005	0.005
Mg	1.850	1.839	1.850	1.863	1.856	1.863	1.867	1.863	1.868	1.749	1.734	1.741
Ca	0.001	0.000	0.000	0.001	0.000		0.000	0.001	0.001	0.000	0.001	0.000
Cr_2O_3	0.004	0.001	0.001			0.000		0.004				
Ni	0.008	0.009	0.009	0.009	0.009	0.008	0.007	0.009	0.010	0.003	0.003	0.004
V		0.001	0.001		0.001	0.001			0.000		0.001	
Total	3.008	3.002	3.006	3.013	3.013	3.017	3.013	3.014	3.015	3.015	3.009	3.014
Fo	92.33	92.33	92.41	92.36	91.97	91.95	92.52	92.37	92.57	86.33	86.10	86.02

Detection limits (ppm): Ti = 213, Al = 101, Mn = 162, Ca = 76, Cr = 1411, Ni = 264, V = 206.

Table 3
Representative chemical analyses (wt% oxides) of orthopyroxene from the La Cocha ultramafic rocks.

Sample	CO 127a	CO 127a	CO 127a	CO 127a	CO 127	CO 127	CO 127	CO 127	CO 118	CO 118	CO 112	CO 112
Point	4	36	43	47	1	2	7	9	17	21	27	38
Total number of orthopyroxene analyses $n = 40$												
SiO_2	56.032	55.799	56.261	56.340	56.896	56.796	56.503	56.852	56.248	57.497	53.534	54.292
TiO_2				0.014	0.021	0.022	0.022	0.010		0.032	0.056	0.041
Al_2O_3	1.158	0.926	1.096	0.987	0.845	1.047	1.125	0.907	1.486	0.489	3.412	3.173
FeO	5.374	5.498	5.476	5.491	5.591	5.523	5.777	5.843	5.572	5.192	9.634	9.871
MnO	0.133	0.097	0.151	0.148	0.135	0.130	0.167	0.162	0.138	0.094	0.240	0.233
MgO	35.036	35.336	35.208	35.313	36.225	36.008	36.013	36.079	36.023	36.108	31.922	32.297
CaO	0.087	0.075	0.095	0.089	0.137	0.141	0.230	0.112	0.148	0.135	0.122	0.120
Na_2O	0.028	0.001	0.036	0.001	0.007	0.023	0.018	0.001	0.011	0.002	0.001	0.023
K_2O	0.007	0.010	0.010	0.010	0.002	0.003	0.006		0.009	0.028	0.004	
Cr_2O_3	0.324	0.348	0.119	0.146	0.152	0.152	0.164	0.100	0.216		0.216	0.160
NiO	0.041	0.057	0.129	0.068	0.077	0.085	0.133	0.085	0.039	0.070	0.035	
V_2O_3	0.007	0.007	0.023	0.028	0.035		0.010	0.035		0.032		
Total	98.23	98.154	98.604	98.64	100.12	99.93	100.17	100.19	99.89	99.68	99.18	100.21
Number of cations on the basis of 6O												
TSi	1.954	1.947	1.955	1.957	1.944	1.944	1.931	1.944	1.925	1.973	1.882	1.889
TAl	0.046	0.038	0.045	0.040	0.034	0.042	0.045	0.037	0.060	0.020	0.118	0.111
TFe_3		0.015		0.003	0.022	0.013	0.023	0.020	0.015	0.008		
M_1Al	0.002										0.023	0.019
M_1Ti					0.001	0.001	0.001			0.001	0.001	0.001
M_1Fe_3	0.037	0.044	0.045	0.039	0.051	0.052	0.065	0.053	0.070	0.027	0.086	0.086
M_1Fe_2												
M_1Cr	0.009	0.010	0.003	0.004	0.004	0.004	0.004	0.003	0.006		0.006	0.004
M_1Mg	0.951	0.945	0.948	0.955	0.942	0.941	0.927	0.942	0.923	0.970	0.883	0.889
M_1Ni	0.001	0.002	0.004	0.002	0.002	0.002	0.004	0.002	0.001	0.002	0.001	
M_2Mg	0.871	0.893	0.875	0.874	0.903	0.897	0.908	0.897	0.915	0.877	0.790	0.786
M_2Fe_2	0.120	0.101	0.114	0.118	0.087	0.093	0.077	0.094	0.075	0.114	0.198	0.201
M_2Mn	0.004	0.003	0.004	0.004	0.004	0.004	0.005	0.005	0.004	0.003	0.007	0.007
M_2Ca	0.003	0.003	0.004	0.003	0.005	0.005	0.008	0.004	0.005	0.005	0.005	0.004
M_2Na	0.002		0.002			0.002	0.001		0.001			0.002
M_2K										0.001		
Total	4.000	4.000	4.000	4.000	4.000	4.000	4.000	4.000	4.000	0.399	4.000	4.000
En	91.744	91.712	91.606	91.624	91.624	91.667	91.140	91.271	91.583	92.180	85.011	84.874

Detection limits (ppm): Ti = 205, Al = 106, Mn = 161, Ca = 75, Na = 123, K = 64, Cr = 1407, Ni = 259, V = 206.

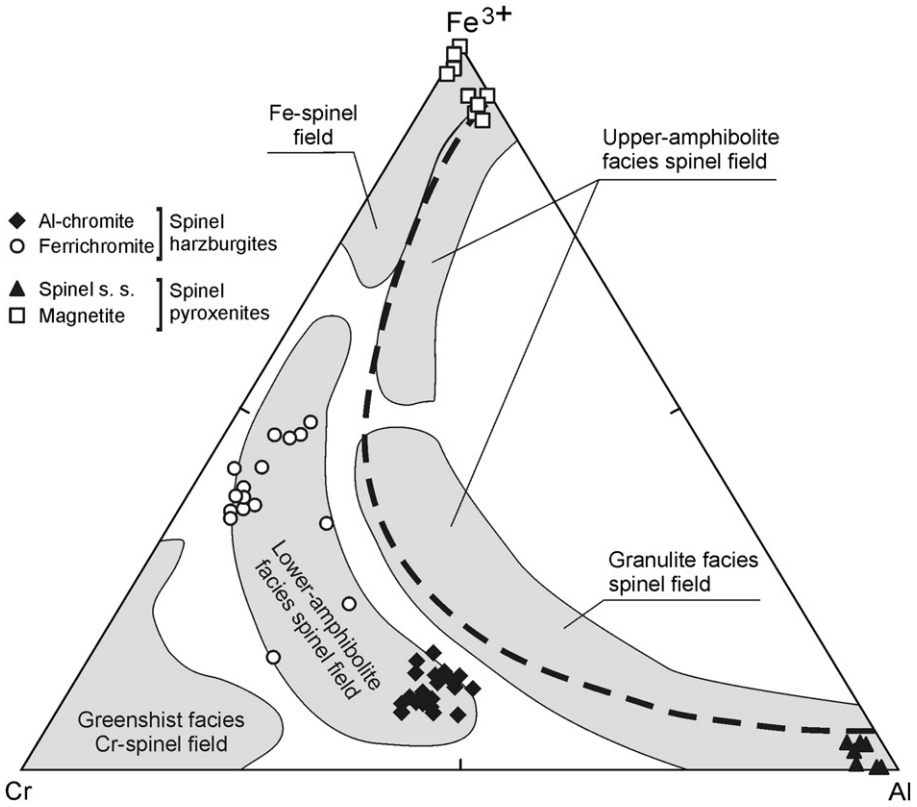

Fig. 4. Spinel compositions from the La Cocha ultramafic rocks based on the trivalent cations Fe^{3+}–Cr–Al. Compositional fields from different metamorphic facies after Evans and Frost (1975) and Suita and Streider (1996). The cut line is the solvus curve for different metamorphic chromo-spinel phases (Purvis et al., 1972; Evans and Frost, 1975; Suita and Strieder, 1996).

4.3. Orthopyroxene

The orthopyroxene in the La Cocha spinel harzburgites has concentrations of 5.1–5.8% of FeO, 34.7–36.1% of MgO, 55.2–56.2% of SiO_2 and 0.8–1.1% of Al_2O_3 (Table 3), with a homogeneous behavior in the analyzed grains, as much from edge to core (intragrain) as in relationship with other grains (intergrain). In some grains, Al_2O_3 content decreases toward the edge (1.5–0.5%; sample Co-118), the same occurs in CaO (0.08–0.12%; samples Co-127 and Co-127a), while MgO can show a light enrichment toward the edge. The analyzed orthopyroxene is plotted in the **enstatite** field (En_{92}) in the diagram Wo–En–Fs for pyroxene classification of Morimoto et al. (1988).

The enstatite component shows a decrease from the spinel harzburgites (En_{92}) to the spinel pyroxenites (En_{85}). In the last ones (sample Co-112), orthopyroxene shows enrichment in FeO (9.60–9.87%) and Al_2O_3 (2.87–3.46%), depletion in SiO_2 (53.42–54.29%) and MgO (31.49–32.36%), with similar concentrations of the other elements, in relationship with the spinel harzburgites.

5. Reactions textures in the minerals of the spinel group

Most Al–chromite grains in the La Cocha spinel harzburgites are unaltered or only show very thin magnetite rims (Fig. 3e,f) produced during the serpentinization of olivine and orthopyroxene. Although, some Al–chromite grains record replacement by ferrichromite (Fig. 3g,h) from grain boundaries or fractures toward the interior of the grains, giving rise to zoned grains consisting of mostly unaltered Al–chromite cores irregularly enveloped by variably thick, ferrichromite rims (Gervilla et al., 2012).

Chromite tends to lose content in Al, relative to Cr, during metamorphism and reaction with silicates and metamorphic fluids to form chlorite or amphibole, increasing the Cr# (Barnes and Roeder, 2001). In the La Cocha spinel harzburgites, loss of Al in spinel generated the transformation of some chromite grains (Al-rich) to ferrichromite (Al-poor), raising the Cr# up to values between 0.83 and 0.94. As a consequence of this process, the compositions of ferrichromite are plotted along the Cr–Fe^{+3} join in the Cr–Al–Fe^{+3} diagram (Fig. 4) and at the top right of the Cr#–Mg# diagram (Fig. 5a). The Al_2O_3–TiO_2 diagram (Fig. 6) shows the decrease of Al_2O_3 contents in spinel by alteration to ferrichromite. The effect of metamorphism in the serpentinized ultramafic rocks is thus mirrored by the mineral chemistry of spinel (arrows in Fig. 5a and Fig. 6).

The Fe^{3+} enrichment in the alteration rim of ferrichromite suggests an oxidative state during metamorphism. Relatively high oxidative conditions favor the reaction of spinel (or the spinel component of chromite) with serpentine to produce chlorite and a Fe-rich, Cr-spinel intermediate between chromite and magnetite (Mellini et al., 2005; González-Jiménez et al., 2009):

$$\left(Fe^{2+}, Mg\right)(Cr, Al)_2O_4 + 1.5\ Mg_3Si_2O_5(OH)_4 + H_2O + 0.083O_2 = MgAlSi_3O_{10}(OH)_8 + 0.167(Fe, Cr)_3O_4$$

$$Al-\text{chromite} + \text{serpentine} + H_2O + O_2 = \text{chlorite} + \text{ferrichromite}.$$

Metamorphism stopped serpentinization of pyroxene and olivine (Frost, 1985; Bach et al., 2006), favoring an oxidizing environment. According to Fig. 4, this alteration event should have

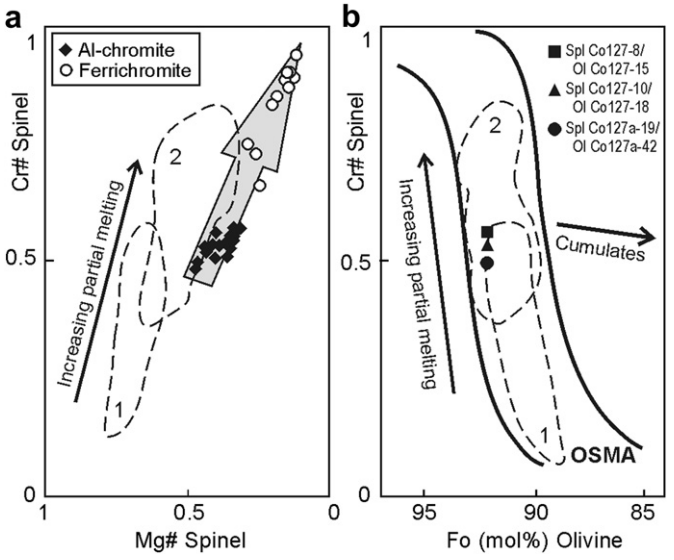

Fig. 5. **a**. Cr-number [Cr# = Cr/(Cr + Al)] versus Mg-number [#Mg = Mg/(Mg + Fe^{2+})] in spinel. **b**. Cr# (in spinel) versus Fo content (in olivine) from the La Cocha spinel harzburgites. The arrow indicates the effect of metamorphism. OSMA: olivine spinel mantle array. Also shown are fields of abyssal or ocean floor peridotites (1) after Dick and Bullen (1984) and Arai (1994b), and forearc peridotites (2) after Bloomer and Hawkins (1983), Bloomer and Fisher (1987), Ishii et al. (1992) and Parkinson and Pearce (1998).

taken place during lower temperature amphibolite facies metamorphism (Purvis et al., 1972; Evans and Frost, 1975; Suita and Streider, 1996). In the studied area, these conditions were reached during the M3 retrograde event recorded in the associated metamorphic rocks (Martino et al., 2010).

The lack of evidence of alteration in Al–chromite during the early stages of the main regional metamorphism recorded in the studied area (M2–D2 metamorphic event, upper amphibolite to granulite facies, Martino et al., 2010) shows either that it was not affected by this metamorphic event or that it was completely obliterated by the subsequent oxidizing M3 event (González-Jiménez et al., 2009). One reason is that the metamorphic modifications of Cr-spinel are controlled by the fluid phases (Candia and Gaspar, 1997; Proenza et al., 2004), so a high-grade metamorphic event with $P_{H_2O} < P_{total}$ as occurs in the studied area could have preserve primary compositions.

In the La Cocha spinel pyroxenites, green spinel shows exsolution textures of magnetite blebs and rims (Fig. 3d). In the Cr–Al–Fe^{+3} triangle (Fig. 4), the spinel (*s. s.*) compositions plot in the Al-rich corner. According to Evans and Frost (1975) and Barnes and Roeder (2001), spinels of these compositions are formed by metamorphic reaction at upper amphibolite to granulite facies conditions. The development of magnetite blebs and rims around spinel (*s. s.*) imply loss of Al and enrichment in Fe, common in many metamorphized ultramafic rocks (see for ex.: Onyeagocha, 1974; Bliss and MacLean, 1975; Abzalov, 1998; Barnes, 2000). In these rocks, the spinel and the magnetite rims delineate two different trains in the Cr–Al–Fe^{+3} triangle (Fig. 4). The scarce green spinel in the harzburgites (in samples that do not contain Al–chromite) are also interpreted as produced by metamorphic reaction.

Based on textural analysis, only the cores of unaltered Al–chromite grains with high MgO and low Fe_2O_3 contents have been considered in the interpretation of the primary phases, and used as petrogenetic indicators.

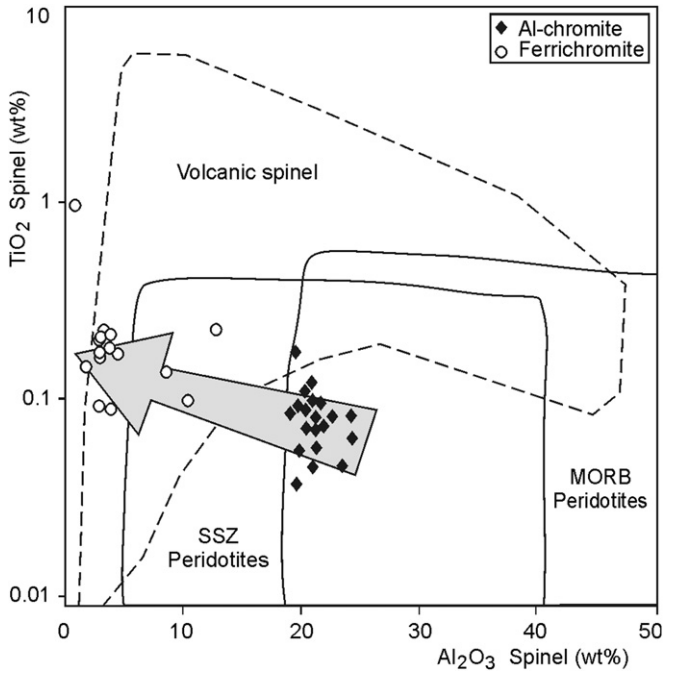

Fig. 6. Discrimination between volcanic and mantle spinel using TiO_2 versus Al_2O_3 from the La Cocha spinel harzburgites. Fields for supra-subduction zone (SSZ) peridotite sand mid-ocean ridge basalts (MORB) peridotites after Kamenetsky et al. (2001). The arrow indicates the effect of metamorphism. Note that TiO_2 is in logarithmic scale.

6. Geothermometry

The geothermometer calibrations of Fàbries (1979), Roeder et al. (1979), Ballhaus et al. (1991), Berger and Vannier (1978), Povdin (1988), Brey and Köhler (1990) and Witt-Eickschen and Seck (1991) were used for the calculation of temperature conditions. The main results obtained using the different geothermometers and their references are listed in Table 4.

To estimate the temperature conditions under which the La Cocha spinel harzburgites may have been equilibrated, geothermometers that include the primary mineral association olivine (Fo_{92}) + orthopyroxene (En_{91-92}) + spinel (Al–chromite) were used. The cores of unaltered grains of olivine, orthopyroxene and Al–chromite are interpreted to represent this primary association. Pressures were not determined; however, spinel-facies peridotites indicate intermediate pressures (10–15 kb). Upper mantle mineral assemblages are usually equilibrated at a pressure of 15 kb (Fabries, 1979) and therefore this value is assumed for temperature

Table 4
Results of the different geothermometers applied to the La Cocha ultramafic rocks.

Spinel harzburgites		Sample	*T* (°C)	Sample	*T* (°C)
Ol-Spl	1 (P = 15 kb)	Co127a	1157	Co127	1090
	2 (P = 15 kb)		903		823
	3 (P = 15 kb)		994		939
Opx-Ol	4	Co127a	921		
	5		796–1053		
Opx	6 (±26 °C)	Co127a	682	Co127	653
	7		726		680
	6	Co127a	618	Co127	682
	7		771		695
Spinel pyroxenites					
Opx	6 (±26 °C)	Co112	785		
	7		734		

References: 1 – Fàbries (1979); 2 – Roeder et al. (1979); 3 – Ballhaus et al. (1991); 4 – Berger and Vannier (1978); 5 – Povdin 1988; 6 – Brey and Köhler (1990); 7 – Witt–Eickschen and Seck (1991).

calculations that require it; calculations at 10 kb show only minor variations (±10 °C).

In the spinel harzburgites, the higher temperatures were determined using calibrations developed for the pairs olivine–spinel (823–1157 °C) and orthopyroxene–olivine (796–1053 °C), while lower temperatures were calculated using geothermometers with orthopyroxene (618–771 °C).

Because of ionic diffusion mechanisms and transfer reactions associated with metamorphic processes can alter the chemical compositions of the minerals used in the experimental temperature calibrations, the highest value obtained of 1157 °C could be considered as valid to estimate the primary conditions in the spinel harzburgites (Esteban et al., 2004). Lower temperature values would be related to subsolidus re-equilibration between some of the mineral phases produced by metamorphism.

In the spinel pyroxenites, temperatures of 785–734 °C were calculated using geothermometers with orthopyroxene. These values are interpreted to be related to metamorphism in amphibolite to granulite facies conditions.

7. Interpretation

The high forsterite content (Fo_{92}) in olivine from the La Cocha spinel harzburgites is consistent with values from harzburgites of the mantle (Deer et al., 1992). The olivine and Al–chromite compositions fall within the mantle array (OSMA, Fig. 5b), which could be interpreted as evidence of the residual origin of these peridotites (Arai, 1994b). These compositions show that olivine did not suffer important modifications and could represent conditions previous to serpentinization and regional metamorphism. The low concentrations of Ni (900–1590 ppm) and Cr (1400–2270 ppm) in whole rock analyses (Anzil, 2009; Anzil and Martino, 2009b) also support the residual origin for these peridotites.

Cumular textures were not observed in outcrops and thin sections of the studied rocks. The narrow and high Fo range (Fig. 5b) is also typical of residual peridotites, particularly harzburgites and dunites, and unlike cumulate rocks which tend to show lower Fo contents (Arai, 1994b; Coish and Gardner, 2004). Pugliese (1995) proposed a cumular origin for the La Cocha peridotites but, in this case, the Fo range should be wider and lower. Besides, on the variation diagram NiO versus Fo content (Fig. 7a), olivine in the La Cocha harzburgites is represented in the 'ophiolites' and 'chromitites' fields, away from the 'cumulates from ophiolites' field. On the variation diagram MnO versus Fo content (Fig. 7b), olivine is also represented in the 'ophiolites' fields, away from the 'cumulates from ophiolites' field, although some points, possibly affected by metamorphism, plot in the 'tremolite-talc' field.

Fig. 7a,b is not conclusive with regard to the origin of the spinel pyroxenites (sample Co-112), in which olivine is plotted among the fields of 'cumulates from ophiolites', 'ophiolites' and 'tremolite-talc'. A possible origin for the La Cocha pyroxenite lenses is attributed to the circulation of mafic flows that reacted with the host harzburgites, which could explain the compositional variations of olivine and orthopyroxene in both rocks. The hornblendites layers that occur in the contact between the amphibolites and the ultramafic body could be interpreted as product of the reaction between a fluid phase and the associated rocks.

Another feature supporting the primary origin of olivine is the elongated shape of the crystals/aggregates (preserved in pseudomorphic replacements; Anzil, 2009; Martino et al., 2010), interpreted as evidence of ductile flow and recrystallization under high temperature conditions in the mantle (Carter and Avé Lallemant, 1970; Schneider et al., 2008).

In the Al_2O_3–TiO_2 diagram (Fig. 6), Al–chromite plots within the typical mantle spinel fields (Kamenetsky et al., 2001), but the tectonic environment of the peridotites is ambiguous. The Cr_2O_3 and TiO_2 contents in spinel are a function of the degree of partial melting suffered by the peridotite (Dick and Bullen, 1984; Arai, 1994b). In the analyzed Al–chromite, the Cr# is lower to 0.6 in all the samples (<0.57, Fig. 5a), which suggest that the rocks suffered partial melting, but not in the degree of highly refractory peridotites with Cr# up to 0.7 (Dick and Bullen, 1984; Arai, 1994b). The

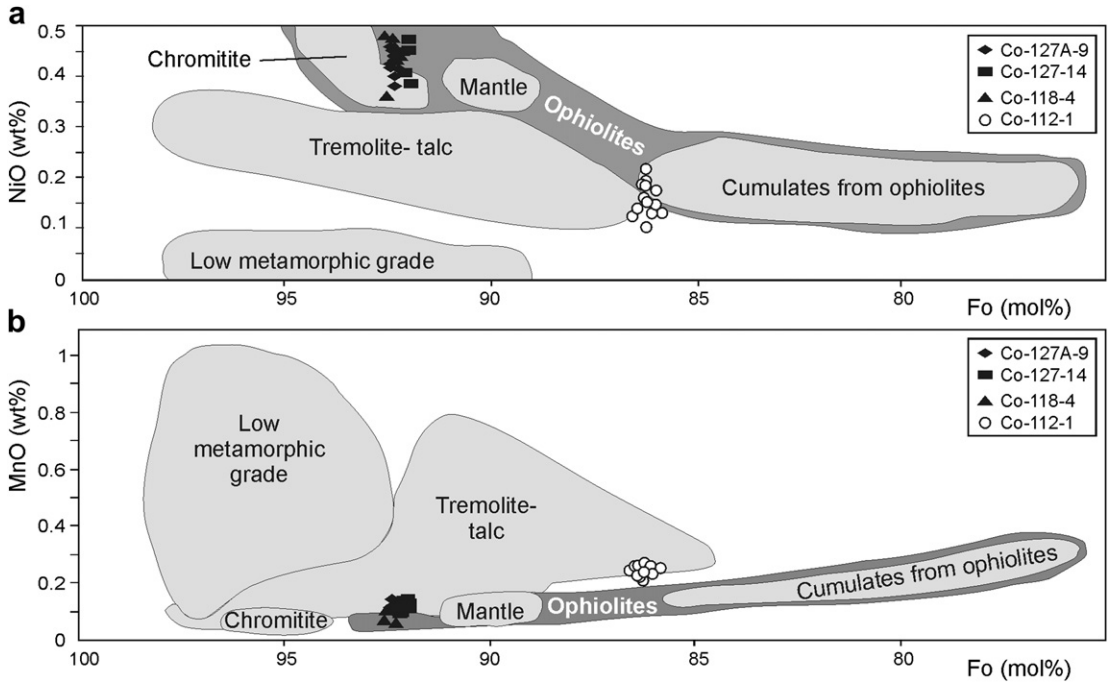

Fig. 7. Variation diagrams of NiO **(a)** and MnO **(b)** versus Fo content in olivine from the La Cocha spinel harzburgites (black symbols) and spinel pyroxenites (white symbols). Compositional fields from Vance and Dungan (1977), modified from Hartmann and Chemale (2003), shown for comparison.

TiO_2–Cr_2O_3 diagram (Fig. 8) for chromitites worldwide confirms this origin for Al–chromite in the La Cocha harzburgites, which fall within the field of depleted oceanic peridotites (tectonites). In the TiO_2–Cr# in spinel diagram (Fig. 9), they fall within the refractory abyssal peridotites field defined by Kelemen et al. (1997).

Aluminum contents in pyroxene are also known to be sensitive to the degree of mantle melting, decreasing systematically with increasing depletion of peridotites (Zhou et al., 2005). The low Al_2O_3 contents of orthopyroxene in the La Cocha spinel harzburgites (0.8–1.2%) are typical of depleted peridotites. The slight compositional variations towards the edge would be produced by metamorphism.

Ahmed et al. (2005) suggest that the production of highly depleted peridotites and related rocks, i.e. the high degree of partial melting, was much more prevalent in the Precambrian time than in the Phanerozoic time.

The high Al content of chromite in the La Cocha harzburgites could indicate that they belong to transition areas between crust and mantle (Zhou and Robinson, 1997; Proenza et al., 1999), while the Cr-rich chromite belong to deeper areas of the mantle sequence.

The association of the La Cocha ultramafic rocks with mafic bodies (amphibolites, Fig. 2) would also support an origin as an oceanic mantle slice: Anzil (2009) and Anzil and Martino (2012) classified the two pyroxene amphibolites as belonging to the tholeiitic series and rare earth elements diagrams suggest a parental magma with an N-type MORB signature. Also, the non-pyroxene amphibolites could belong to an N-type MORB environment, with low contents of light rare earth elements, suggesting that their parental melt has originated from a depleted mantle.

8. Metamorphic evolution of the ultramafic rocks

The thermotectonic evolution of the metamorphic rocks in the studied area was established by Martino et al. (2010) based on the petrography, geothermobarometry and structure of high grade gneisses associated with the ultramafic bodies in the Sierra Chica of Córdoba. The paragenesis of the ultramafic rocks were established by Anzil (2009) and the serpentine replacements by Anzil and Martino (2009b).

The ultramafic rocks recorded high-temperature mantle events developed during a precontinental stage, preserving primary relics of olivine, orthopyroxene and Al–chromite, and a mantle foliation. Pseudomorphic replacements of olivine and orthopyroxene by lizardite + magnetite, without Al–chromite alteration, were associated with ocean-floor metamorphism. This event was previous to the Pampean orogenic cycle (Prepampean), constrained by Sm/Nd

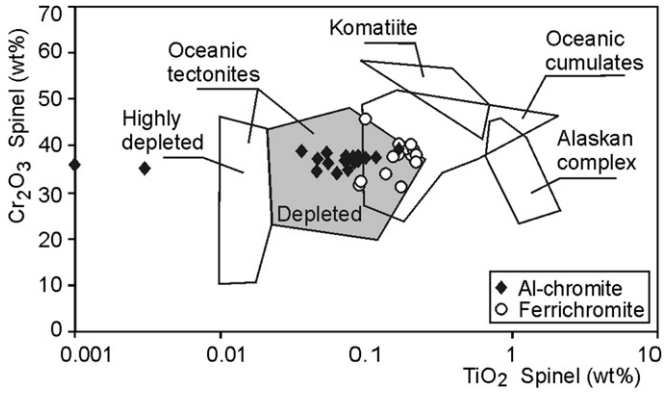

Fig. 8. Diagram Cr_2O_3–TiO_2 in spinel from the La Cocha spinel harzburgites. Fields of ultramafic rocks after Herbert (1982), Jan and Windley (1990), Zhou and Kerrich (1992). Note that TiO_2 is in logarithmic scale.

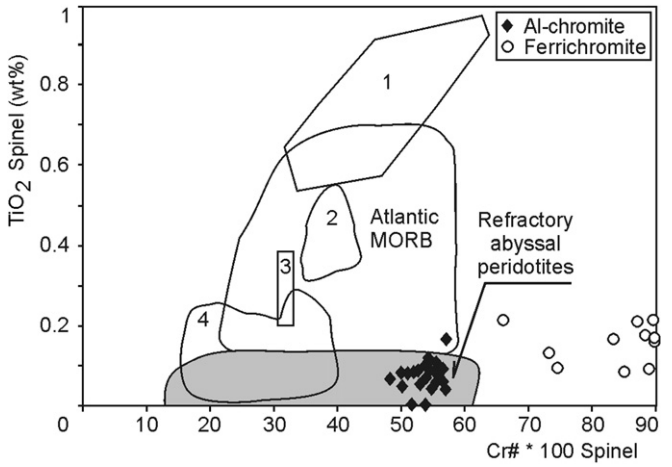

Fig. 9. Diagram TiO_2–Cr# in spinel from the La Cocha spinel harzburgites. Fields of refractory abyssal peridotites and Atlantic MORB after Kelemen et al. (1997). References: 1 – plagioclase peridotites; 2 – replacive spinel dunites; 3 – replacive spinel harzburgites; 4 – reactive spinel peridotites.

ages (647 ± 77 Ma; Escayola et al., 2007) from ultramafic bodies in the Sierra Grande of Córdoba.

After the tectonic emplacement of the ultramafic bodies, during a continental stage (Pampean Cycle, ~530 Ma; Rapela et al., 1998; Siegesmund et al., 2010), the main M2–D2 regional metamorphism (Martino et al., 1995, 1997, 1999, 2010) under high amphibolite to granulite facies conditions occurred. In the ultramafic rocks, it was recorded by the development of disseminated amphibole and clinochlore (±ferrichromite) in the serpentine matrix. Chrysotile occurs in non-pseudomorphic textures and diffuse bastites. The breakdown of spinel could begin in this event. A previous M1–D1 event is only recorded by relict textures in the associated high-grade gneisses.

A strong D3 constrictional deformation in a simple shear regime under high-temperature conditions affected the ultramafic bodies forming tubular sheath folds. Later, a M3 retrograde metamorphism, under amphibolite facies conditions, took place. In the ultramafic rocks, corona textures composed of ferrichromite, magnetite and a new clinochlore around some Al–chromite grains were developed. Serpentinized (lizardite) edges in the previously formed amphibole and clinochlore also occur. Veins of lizardite and tremolite (±clinochlore) developed along an axial plane foliation. During a last M4 event, veins that cut all the minerals, composed of calcite, clinochlore, chrysotile or talc, were produced by low-temperature fluids in the ultramafic rocks.

Based on local and regional structural relationships, Martino et al. (2010) interpreted that the Sierra Chica ultramafic bodies were emplaced as upper mantle slices in an accretionary prism that was reworked during the Pampean orogeny, preserving its primary mineral phases as relics, and that the same outcrop-pattern can also be recognized in the other ultramafic bodies of the Sierras de Córdoba. The La Cocha ultramafic body shows similar petrological, geochemical and structural features than the other ultramafic bodies in the Sierras de Córdoba (Martino et al., 2010, and references therein), therefore the origin as an oceanic mantle slice proposed here could be considered to interpret the other ultramafic bodies in the Sierras de Córdoba.

9. Conclusions

In the La Cocha spinel harzburgites, the primary spinel is Al–chromite (Cr# = 0.48–0.57), which was replaced by ferrichromite

and chlinoclore by metamorphism. Orthopyroxene is enstatite (En_{92}) and olivine is classified as forsterite (Fo_{92}), this last one with a homogeneous and constant composition along the body. Geothermometric calculations using the pair olivine–spinel gave temperatures of 1157 °C, which would correspond to the primary conditions of formation of the harzburgites.

The spinel pyroxenites show a mineral composition defined by orthopyroxene (En_{85}, enstatite), olivine (Fo_{86}, chrysolite), spinel (*s. s.*) and magnetite. Serpentine and clinochlore were products of metamorphism. Spinel has high concentrations in Al and very low in Cr, and is classified as spinel *sensu stricto*; blebs and rims of magnetite were produced by metamorphism. Orthopyroxene and olivine are depleted in MgO regarding these minerals in the harzburgites. Temperatures of 785–734 °C calculated using geothermometers with orthopyroxene are interpreted to be produced by metamorphism in amphibolite to granulite facies conditions.

The narrow composicional range and high forsterite content in olivine, the high Cr content in spinel, and the low concentrations of Ni and Cr in whole rock analyses indicate a mantle residual origin for the studied peridotites, which would exclude a cumular origin for these rocks.

The association of the peridotites with mafic bodies formed in an N-type MORB environment and the relict mantle fabric showed by the crystals/aggregates of olivine, indicating a high temperature flow, allow to interpret the La Cocha ultramafic body as a slice of oceanic mantle, belonging to basal tectonites of an ophiolite complex.

The La Cocha ultramafic body shows similar petrological, geochemical and structural features than the other ultramafic bodies in the Sierras de Córdoba, therefore the origin as an oceanic mantle slice proposed here could probably be applied to the other ultramafic bodies in the Sierras de Córdoba.

Acknowledgments

The authors thank Argentina Research Agencies (FONCyT PICT–R N° 179, CONICET PIP 6310 and SECyT–UNC I500) for granting analytical facilities and field trips. Also thank A. Castro (Departamento de Geología, Universidad de Huelva, Spain) for facilitate the access to the microprobe. Anonymous reviewers helped to improve the manuscript.

References

Abzalov, M., 1998. Chrome–spinels in gabbro–wehrlite intrusions of the Pechenga area, Kola Peninsula, Russia: emphasis on alteration features. Lithos 43, 109–134.

Ahmed, A.H., Arai, S., Abdel-Aziz, Y.M., Rahimi, A., 2005. Spinel composition as a petrogenetic indicator of the mantle section in the Neoproterozoic Bou Azzer ophiolite, Anti-Atlas, Morocco. Precambrian Research 138, 225–234.

Anzil, P., 2009. Metamorfismo, deformación y evolución tectónica de rocas ultramáficas y su encajonante metamórfico asociado en la Sierra Chica Central, Córdoba, Argentina. Tesis Doctoral, Hemeroteca de la Facultad de Ciencias Exactas, Físicas y Naturales, Universidad Nacional de Córdoba, p. 336 (unpublished).

Anzil, P., Martino, R., 2009a. The megascopic and mesoscopic structure of La Cocha ultramafic body, Sierra Chica of Córdoba, Argentina. Journal of South American Earth Sciences 28, 398–406.

Anzil, P.A., Martino, R.D., 2009b. Aspectos geoquímicos relacionados a la serpentinización y anfibolitización del cuerpo ultramáfico de La Cocha, Sierra Chica, Córdoba. Revista de la Asociación Geológica Argentina 65 (3), 468–478.

Anzil, P.A., Martino, R.D., 2012. Petrografía y geoquímica de las anfibolitas del cerro La Cocha, Sierra Chica, Córdoba. Revista de la Asociación Geológica Argentina 69 (2), 261–272.

Arai, S., 1992. Chemistry of chromian spinel in volcanic rocks as a potential guide to magma chemistry. Mineralogical Magazine 56, 173–184.

Arai, S., 1994a. Characterization of spinel peridotites by olivine–spinel compositional relationships; review and interpretation. Chemical Geology 113, 191–204.

Arai, S., 1994b. Compositional variation of olivine chromian spinel in Mg-rich magmas as a guide to their residual spinel peridotites. Journal of Volcanology and Geothermal Research 59, 279–293.

Bach, W., Paulick, H., Garrido, C.J., Ildefonse, B., Meurer, W., Humphris, S.E., 2006. Unravelling the sequence of serpentinization reactions: petrography, mineral chemistry, and petrophysics of serpentinites from MAR 15°N (ODP Leg 209, Site 1274). Geophysical Research Letters 25, 1467–1470.

Ballhaus, C., Berry, R., Green, D., 1991. High pressure experimental calibration of the olivine–orthopyroxene–spinel oxygen geobarometer: implications for the oxidation state of the upper mantle. Contribution Mineralogy and Petrology 107 (1), 27–40.

Barnes, S., 2000. Chromite in komatiites, II. Modification during greenschist to mid-amphibolite facies metamorphism. Journal of Petrology 41, 387–409.

Barnes, S., Roeder, P., 2001. The range of spinel composition in terrestrial mafic and ultramafic rocks. Journal of Petrology 42 (12), 2279–2302.

Barra, F., Rabbia, O.M., Alfaro, G., Miller, H., Höfer, C., Kraus, S., 1998. Serpentinitas y cromititas de La Cabaña, Cordillera de la Costa, Chile central. Revista Geológica de Chile 25 (1), 29–44.

Berger, E., Vannier, M., 1978. Un géothermométre reposant sur le partage du nickel et du magnésium entre olivine et orthopyroxéne: Application a l'étude des peridotites. Comptes Rendus de l'Académie des Sciences de Paris, Serie D 86 (2), 733–736.

Bliss, N., MacLean, W., 1975. The paragenesis of zoned chromite from central Manitoba. Geochimica et Cosmochimica Acta 39, 973–990.

Bloomer, S.H., Fisher, R.L., 1987. Petrology and geochemistry of igneous rocks from the Tonga Trench – a non accreting plate boundary. Journal of Geology 95, 469–495.

Bloomer, S., Hawkins, J., 1983. Gabbroic and ultramafic rocks from the Mariana Trench: an Island Arc Ophiolite. In: Hayes, D. (Ed.), The Tectonics and Geologic Evolution of Southeast Asian Seas and Islands (Part II). American Geophysical Union, Washington, pp. 294–317.

Brey, G., Köhler, T., 1990. Geothermobarometry in four phase lherzolites II. New thermobarometers and practical assessment of existing thermobarometers. Journal of Petrology 31, 1353–1378.

Candia, M.A.F., Gaspar, J.C., 1997. Chromian spinels in metamorphosed ultramafic rocks from Mangabal I and II complexes, Goiás, Brazil. Mineralogy and Petrology 60, 27–40.

Carter, N., Avé Lallemant, H., 1970. High temperature deformation of dunite and peridotite. Geological Society of America Bulletin 81, 2181–2202.

Coish, R., Gardner, P., 2004. Suprasubduction-zone peridotite in the northern USA Appalachians: evidence from mineral composition. Mineralogical Magazine 68 (4), 699–708.

Deer, W., Howie, R., Zussman, J., 1992. An Introduction to the Rock-forming Minerals, second ed. Longman Scientific and Technical, p. 696.

Dick, H., Bullen, T., 1984. Chromian spinel as a petrogenetic indicator in abyssal and alpine-type peridotites and spatially associated lavas. Contributions to Mineralogy and Petrology 86, 54–76.

Duncan, R., Green, D., 1980. Role of multistage melting in the formation of oceanic crust. Geology 8, 22–26.

Escayola, M.P., Kraemer, P.E., 2003. Significado geotectónico de las suturas de Sierras Pampeanas Orientales en la faja orogénica Córdoba: Posible correlación con orógenos brasilianos. Revista Brasileira de Geociências 33 (1–Suplemento), 69–76.

Escayola, M.P., Ramé, G., Kraemer, P.E., 1996. Caracterización y significado geotectónico de las fajas ultramáficas de las Sierras Pampeanas de Córdoba. In: 13° Congreso Geológico Argentino and 3° Congreso de Exploración de Hidrocarburos, Buenos Aires, Actas 3, pp. 421–438.

Escayola, M.P., Pimentel, M., Armstrong, R., 2007. Neoproterozoic backarc basin: sensitive high-resolution ion microprobe U–Pb and Sm–Nd isotopic evidence from Eastern Pampean Ranges, Argentina. Geology 35 (6), 495–498.

Esteban, J., Cuevas, J., Tubías, J., 2004. Secuencia microestructural de las peridotitas del macizo ultramáfico de Carratraca (Málaga). Revista de la Sociedad Geológica de España 17 (1–2), 103–115.

Evans, B., Frost, B., 1975. Chrome spinel in progressive metamorphism: a preliminary analysis. Geochimica et Cosmochimica Acta 39, 379–414.

Fàbries, H., 1979. Spinel–olivine geothemtometry in peridotites from ultramafic complexes. Contributions to Mineralogy and Petrology 69 (3), 329–336.

Frost, B.R., 1985. On the stability of sulfides, oxides and native metals in serpentinite. Journal of Petrology 26, 31–63.

Gervilla, F., 1997. Paragénesis de alteración de rocas ultramáficas: serpentinización. In: Melgarejo, J.-C. (Ed.), Atlas de Asociaciones Minerales en Lámina Delgada. Edicions Universitat de Barcelona, Fundació Folch, Barcelona, pp. 91–97.

Gervilla, F., Padrón-Navarta, J.A., Kerestedjian, T., Sergeeva, I., González-Jiménez, J.M., Fanlo, I., 2012. Formation of ferrian chromite in podiform chromitites from the Golyamo Kamenyane serpentinite, Eastern Rhodopes, SE Bulgaria: a two-stage process. Contributions to Mineralogy and Petrology. http://dx.doi.org/10.1007/s00410-012-0763-3.

González-Jiménez, J.M., Kerestedjian, T., Proenza, J.A., Gervilla, F., 2009. Metamorphism on chromite ores from the Dobromirtsi ultramafic Massif, Rhodope Mountains (SE Bulgaria). Geologica Acta 7 (4), 413–429.

Hartmann, L., Chemale, F., 2003. Mid amphibolite facies metamorphism of harzburgites in the Neoproterozoic Cerro Mantiqueiras Ophiolite, southernmost Brazil. Anais da Academia Brasileira de Ciencias 75 (1), 109–128.

Herbert, R., 1982. Petrography and mineralogy of oceanic peridotites and gabbros: some comparisons with ophiolite examples. Ofioliti 7, 299–324.

Irvine, T., 1965. Chromian spinel as a petrogenetic indicator. Part 1. Theory. Canadian Journal of Earth Sciences 2, 648–671.

Irvine, T., 1967. Chromian spinel as a petrogenetic indicator. Part 2. Petrologic applications. Canadian Journal of Earth Sciences 4, 71–103.

Ishii, T., Robinson, P., Maekawa, H., Fiske, R., 1992. Petrological studies of peridotites from diapiric serpentinite seamounts in the Isu–Ogasawara–Mariana forearc, Leg 125. In: Fryer, P., Pearce, J., Stokking, L. (Eds.), Proceedings of the Ocean Drilling Program, Scientific Results, vol. 125. Ocean Drilling Program, College Stations, TX, pp. 445–485.

Ishiwatari, A., Sokolov, S., Vysotskiy, S., 2003. Petrological diversity and origin of ophiolites in Japan and Far East Russia with emphasis on depleted harzburgite. In: Dilex, Y. (Ed.), Ophiolites in Earth History. In: Robinson, P. (Ed.),, Geological Society of London, Special Publication, vol 218, pp. 597–617.

Jan, M., Windley, B., 1990. Chromian spinel silicate chemistry in ultramafic rocks of the Jijal complex, northwest Pakistan. Journal of Petrology 31, 667–715.

Kamenetsky, V., Crawford, A., Meffre, S., 2001. Factors controlling chemistry of magmatic spinel: an empirical study of associated olivine, Cr–spinel and melt inclusions from primitive rocks. Journal of Petrology 42, 655–671.

Kelemen, P.B., Hirth, G., Shimizu, N., Spiegelman, M., Dick, H.J.B., 1997. A review of melt migration processes in the adiabatically upwelling mantle beneath oceanic spreading ridges. Philosophical Transactions of the Royal Society of London, Series A 355, 283–318.

Kraemer, P.E., Escayola, M.P., Martino, R.D., 1995. Hipótesis sobre la evolución tectónica neoproterozoica de las Sierras Pampeanas de Córdoba (30° 40′–32° 40′ LS), Argentina. Revista de la Asociación Geológica Argentina 50, 47–59.

Loferski, P., Lipin, B., 1983. Exsolution in metamorphosed chromite from the Red Lodge district, Montana. American Mineralogist 68, 777–789.

Martino, R.D., 2003. Las fajas de deformación dúctil de las Sierras Pampeanas de Córdoba: una reseña general. Revista de la Asociación Geológica Argentina 58 (4), 549–571.

Martino, R.D., Kraemer, P., Escayola, M., Giambastiani, M., Arnosio, M., 1995. Transecta de las Sierras Pampeanas de Córdoba a los 32° LS. Revista de la Asociación Geológica Argentina 50 (1–4), 60–77.

Martino, R.D., Guereschi, A.B., Sfragulla, J.A., 1997. Las anatexitas y las vetas auríferas de Río Hondo, sector sudoriental del Macizo de San Carlos, Córdoba, Argentina. Revista de la Asociación Geológica Argentina 52 (4), 433–450.

Martino, R.D., Guereschi, A.B., Sfragulla, J.A., 1999. Los pliegues no cilíndricos de Sagrada Familia y su significado en la evolución deformacional del Macizo de San Carlos, Córdoba, Argentina. Revista de la Asociación Geológica Argentina 54 (2), 139–151.

Martino, R.D., Guereschi, A.B., Anzil, P.A., 2010. Metamorphic and tectonic evolution at the 31° 36′ S across a deep crustal zone from the Sierra Chica of Córdoba, Sierras Pampeanas, Argentina. Journal of South American Earth Sciences 30, 12–28.

Mellini, M., Rumori, C., Viti, C., 2005. Hydrothermally reset magmatic spinels in retrograde serpentinites: formation of "ferritchromit" rims and chlorite aureoles. Contribution to Mineralogy and Petrology 149, 266–275.

Metzger, E., Miller, R., Harper, G., 2002. Geochemistry and tectonic setting of the ophiolitic Ingalls Complex, North Cascades, Washington: Implications for correlations of Jurassic Cordilleran ophiolites. Journal of Geology 110, 543–560.

Morimoto, N., Fabries, J., Ferguson, A.K., Ginzburg, I.V., Ross, M., Seifert, F.A., Zussman, J., Aoki, K., Gottardi, G., 1988. Nomenclature of pyroxenes. American Mineralogist 73, 1123–1133.

Onyeagocha, A., 1974. Alteration of chromite from the Twin Sisters dunite, Washington. American Mineralogist 59, 608–612.

Parkinson, I., Pearce, J., 1998. Peridotites from the Izu–Bonin–Mariana forearc (ODP Leg 125): evidence for mantle melting and melt–mantle interaction in a suprasubduction zone setting. Journal of Petrology 39, 1577–1618.

Pearce, J., Lippard, S., Roberts, S., 1984. Characteristics and tectonic significance of supra-subduction zone ophiolites. In: Kokelaar, B., Howells, M. (Eds.), Marginal Basin Geology. Geological Society London, Special Publication, vol. 16, pp. 77–94.

Pouchou, J., Pichoir, F., 1985. PAP $\phi(\rho z)$ procedure for improved quantitative microanalysis. In: Armstrong, J.T. (Ed.), Microbeam Analysis. San Francisco Press, Inc., San Francisco, California, USA, p. 104.

Povdin, P., 1988. Ni–Mg partitioning between synthetic olivines and orthopyroxenes: application to geothermometry. American Mineralogist 73 (3/4), 274–280.

Proenza, J.A., Gervilla, F., Melgarejo, J.C., Bodinier, J.L., 1999. Al and Cr rich chromitites from the Mayarí–Baracoa Ophiolitic Belt, (eastern Cuba): consequence of interaction between volatile-rich melts and peridotite in suprasubduction mantle. Economic Geology 94, 547–566.

Proenza, J.A., Ortega-Gutiérrez, F., Camprubí, A., Tritlla, J., Elías-Herrera, M., Reyes-Salas, M., 2004. Paleozoic serpentinite enclosed chromitites from Tehuitzingo, (Acatlán complex, southern Mexico): a petrological and mineralogical study. Journal of South American Earth Sciences 16, 649–666.

Pugliese, L., 1995. Geoquímica y petrogénesis del complejo máfico–ultramáfico estratificado del Cerro La Cocha de Bosque Alegre, en la Sierra Chica de Córdoba. Tesis Doctoral, Hemeroteca de la Facultad de Ciencias Exactas, Físicas y Naturales, Universidad Nacional de Córdoba, p. 340 (unpublished).

Pugliese, L., Villar, M., 2001. El complejo máfico-ultramáfico estratificado del Cerro La Cocha, Departamento de Punilla, Provincia de Córdoba. 9° Congreso Latinoamericano de Geología, Actas 1, Montevideo, pp. 5–15.

Pugliese, L., Villar, M., 2002. Aspectos petrológicos y geoquímicos del complejo máfico–ultramáfico estratificado del Cerro La Cocha, Provincia de Córdoba, Argentina. 6° Congreso de Mineralogía y Metalogenia, Actas 1, Buenos Aires, pp. 353–360.

Pugliese, L., Villar, M., 2004. Elementos del grupo del platino en el complejo máfico–ultramáfico del Cerro La Cocha, Departamento de Punilla, Provincia de Córdoba. 7° Congreso de Mineralogía y Metalogenia, Actas 1, Río Cuarto, pp. 119–120.

Purvis, A., Nesbitt, R., Hallberg, J., 1972. The geology of part of the Carr Boyd Rocks complex. Economic Geology 67, 1093–1113.

Ramos, V., Escayola, M., Mutti, D., Vujovich, G., 2000. Proterozoic–early Paleozoic ophiolites of the Andean basement of southern South America. In: Dilek, Y., Moores, E., Nicolas, A. (Eds.), Ophiolites and Oceanic Crust: New Insights from Fields Studies and the Ocean Drilling Program. Geological Society of America, Special Paper, vol. 349, pp. 331–349.

Rapela, C.W., Pankhurst, R.J., Casquet, C., Baldo, E., Saavedra, J., Galindo, C., Fanning, C.M., 1998. The Pampean Orogeny of the southern proto-Andes: Cambrian continental collision in the Sierras de Córdoba. In: Pankhurst, R.J., Rapela, C.W. (Eds.), The Proto-andean Margin of Gondwana. Geological Society of London, Special Publications, vol. 142, pp. 181–217.

Roeder, P.L., 1994. Chromite: from the fiery rain of chondrules to the Kilauea Iki lava lake. Canadian Mineralogist 32, 729–746.

Roeder, P., Campbell, J., Jamieson, H., 1979. A re-evaluation of the olivine–spinel geothermometer. Contributions to Mineralogy and Petrology 68, 325–334.

Schneider, S., Demouchy, S., Kohlstedt, D., 2008. Flow laws describing deformation of the lithospheres of terrestrial planets based on experiments on single crystals of olivine at low temperature and high pressure. Lunar and Planetary Science 39 (1227), 1–2.

Siegesmund, S., Steenken, A., Martino, R., Wemmer, K., López de Luchi, M., Frei, R., Presnyakov, S., Guereschi, A., 2010. Time constraints on the tectonic evolution of Eastern Sierras Pampeanas (Central Argentina). International Journal of Earth Sciences (Geologische Rundschau) 99, 1199–1226.

Spangenberg, K., 1943. Die Chromitlagerstate von Tampadel am Zobten. Zeitschrift fur praktische Geologie 5, 13–35.

Suita, M., Strieder, A., 1996. Cr–spinels from Brazilian mafic–ultramafic complexes: metamorphic modifications. International Geology Review 38 (3), 245–267.

Vance, J., Dungan, M., 1977. Formation of peridotites by deserpentinization in the Darrington and Sultan areas, Cascade Mountains, Washington. Geological Society of America 88, 1497–1508.

Villar, L., 1975. Las fajas y otras manifestaciones ultramáficas de la república Argentina y su significado metalogenético. In: 2° Congreso Iberoamericano de Geología Económica, Actas 3, Buenos Aires, pp. 135–155.

Wicks, F., Whittaker, E., 1977. Serpentine textures and serpentinization. The Canadian Mineralogist 15, 459–488.

Witt-Eikschen, G., Seck, H., 1991. Solubility of Ca and Al in orthopyroxene from spinel peridotite: an improved version of an empirical geothermometer. Contributions to Mineralogy and Petrology 106, 431–439.

Zhou, M., Kerrich, R., 1992. Morphology and composition of chromite in komatiites from the Belingwe Greenstone Belt, Zimbabwe. Canadian Mineralogist 30, 303–317.

Zhou, M.F., Robinson, P.T., 1997. Origin and tectonic environment of podiform chromite deposits. Economic Geology 92, 259–262.

Zhou, M.F., Robinson, P.T., Malpas, J., Edwards, S.J., Qi, L., 2005. REE and PGE geochemical constraints on the formation of dunites of Luobusa ophiolite, Southern Tibet. Journal of Petrology 46, 615–639.